

UNCLASSIFIED

Defense Technical Information Center
Compilation Part Notice

ADP013353

TITLE: Comparison of Microwave Dielectric Properties of between [001] and [011] Ferroelectric Ba[1-x]Sr[x]TiO₃ Thin Films Grown by Pulsed Laser Deposition

DISTRIBUTION: Approved for public release, distribution unlimited

This paper is part of the following report:

TITLE: Materials Research Society Symposium Proceedings; Volume 720. Materials Issues for Tunable RF and Microwave Devices III Held in San Francisco, California on April 2-3, 2002

To order the complete compilation report, use: ADA410712

The component part is provided here to allow users access to individually authored sections of proceedings, annals, symposia, etc. However, the component should be considered within the context of the overall compilation report and not as a stand-alone technical report.

The following component part numbers comprise the compilation report:
ADP013342 thru ADP013370

UNCLASSIFIED

Comparison of Microwave Dielectric Properties of between (001) and (011) Ferroelectric $\text{Ba}_{1-x}\text{Sr}_x\text{TiO}_3$ Thin Films grown by Pulsed Laser Deposition

Seung Eon Moon, Eun-Kyoung Kim, Su-Jae Lee, Seok-Kil Han¹, Kwang-Yong Kang, and Won-Jeong Kim

Wireless Communication Devices Department, Electronics and Telecommunications Research Institute, Taejeon, 305-350, Korea.

¹Rfrtron Co., Ltd, Seoul, 151-050, Korea.

ABSTRACT

The effects of anisotropic dielectric properties of ferroelectric $\text{Ba}_{1-x}\text{Sr}_x\text{TiO}_3$ (BST) films on the characteristics of phase shifter have been studied in microwave regions at room temperature. Ferroelectric BST films with (001) and (011) orientation were epitaxially grown on (001) and (011) MgO substrates, respectively, by pulsed laser deposition method. The structures of BST films were investigated using x-ray diffraction measurement. The microwave properties of orientation engineered BST films were investigated using coplanar waveguide transmission lines that were fabricated on BST films using a thick metal layer by photolithography and etching process. The measured differential phase shift and insertion loss (S_{21}) for (011) BST films are larger than those for (001) BST films. Dielectric constants of the ferroelectric BST films are calculated from the measured S_{21} using a modified conformal-mapping model.

INTRODUCTION

Tunable microwave devices using ferroelectric thin films has been proposed for long time to take advantage of the electric field dependent dielectric constant of the ferroelectricity, which may have advantages over other materials, such as semiconductors and ferrites[1]. Ferroelectric thin films, especially $(\text{Ba}_{1-x}\text{Sr}_x)\text{TiO}_3$ (BST), have been extensively investigated to explore the possibility of the microwave tunable devices. Nevertheless such a great effort, realization of the device is not achieved yet. To realize this feature, we need that ferroelectrics exhibit with a large dielectric constant change with a relatively low external bias field, and a low microwave loss.

The dielectric properties measured at microwave frequencies for BST films deposited by various deposition method have been reported to be affected by many factors, such as oxygen vacancies, strain and stress between films and substrates (due to lattice mismatch and the thermal expansion difference between the films and the substrates), film thickness, grain size, dopant type, Ba/Sr ratio. To attain these goals, several topics have been studying by many groups such as multi-layers, doping, making composite, high temperature annealing, compensating Ba/Sr deficiencies etc[2-12].

Thin film cubic perovskites have been known to be under stressed status because of lattice mismatch between film and substrate[13]. Furthermore, dielectric properties of distorted film are expected to be anisotropic, since polarizations in the cubic and non-cubic is different. To understand more for ferroelectricity, orientation dependent dielectric properties of the ferroelectric thin film is very important[14].

In this paper, we present studies of the effect of the film orientation on the microwave dielectric properties of epitaxially grown BST films on MgO (001) and (011) single crystals by pulsed laser deposition (PLD), respectively.

EXPERIMENTAL DETAILS

Epitaxial (001) and (011) BST films were deposited onto (001) and (011) MgO single crystals by PLD, respectively. A focused pulse laser from a Kr:F eximer gas laser ($\sim 2\text{J}/\text{mm}^2$) transfer the materials of stoichiometric $(\text{Ba}_{0.6}\text{Sr}_{0.4})\text{TiO}_3$ to the heated substrate attached on heater. The oxygen pressure in the deposition chamber was fixed at 200 mTorr, while the substrate temperature was maintained at 825°C . The structural properties of BST films were characterized by x-ray diffraction (XRD) measurement using a Rigaku x-ray diffractometer equipped with $\text{Cu K}\alpha$ radiator source and a 4-circle X-ray diffractometer. The thickness of the deposited BST films was about 420 nm, which was confirmed by a cross sectional scanning electron microscope (SEM). Microwave dielectric properties of the BST films were measured by a HP 8510C network analyzer at frequency range of 0.05-20 GHz using coplanar waveguide (CPW) type phase shifters fabricated from a thick Au electrode (about $2\text{ }\mu\text{m}$) with a thin Cr adhesion layer. The gap width between center and ground electrodes is $7\text{ }\mu\text{m}$, while the center conductor width is fixed at $20\text{ }\mu\text{m}$. The physical length of the BST CPW device is 3 mm. A DC bias field between center and ground electrodes to control the dielectric constant of BST film is applied through bias tees to protect the HP 8510C network analyzer. Coaxial cables and equipment were calibrated up to the microwave picoprobes to minimize measurement uncertainty using a commercial standard kit. Dielectric constants were extracted using a modified conformal-mapping model from the measured S_{21} and dimension of the CPW[15,16].

DISCUSSION

Though the structural properties of the BST thin films are strongly dependent on the direction of the substrate, growth condition of the films are critical to get epitaxial film without secondary orientations. Epitaxial BST film growth on (001) MgO were achieved in broad deposition conditions; heater temperature higher than 650°C , and oxygen pressure between 50 to 500 mTorr. The higher heater temperature leads the better thin film quality and epitaxiality.

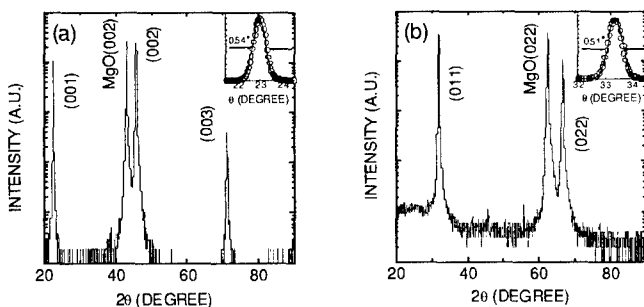


Figure 1. X-ray θ - 2θ diffraction scan patterns of (a) (001) and (b) (011) BST/MgO, respectively. The insets show the XRD ω -rocking curve from the BST (002) and BST (022) of (001) and (011) BST films, respectively.

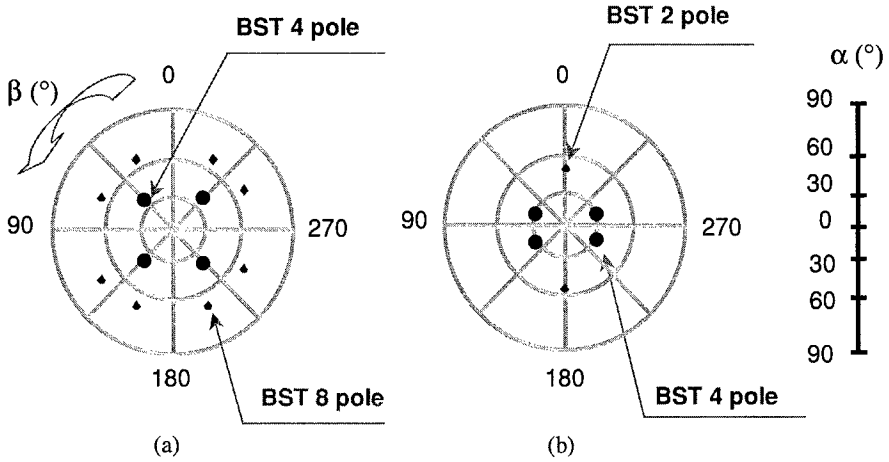


Figure 2. X-ray diffraction pole figure plots of the $\{112\}$ reflections for (a) (001) and (b) (011) BST film deposited on (001) and (011) MgO substrate, respectively.

Furthermore oxygen pressure higher than 500 mTorr lead nucleation of the secondary orientations, such as (011), and (111). BST films grown on (011) MgO exhibit a narrower deposition conditions than those on (001) MgO. Deposition temperature higher than 800 °C shows a negligible intensity of (001) orientation. At 825 °C, epitaxial (011) BST film with 200 mTorr of oxygen pressure was grown successfully without other intensities. Epitaxial growth of each BST films on (001) and (011) MgO single crystals were confirmed by 4-circle diffractometer before fabricating devices. The XRD patterns of (001) and (011) oriented BST films on (001) and (011) MgO substrates, respectively, are shown in fig. 1. Secondary orientations are not shown in both XRD patterns, which suggest that each BST film is oriented along one direction and single phase. The insets in fig. 1 show the XRD ω -rocking curves from the BST (002) and BST (022) of (001) and (011) BST films, respectively. The full width half maximum (FWHM) values for (001) and (011) BST films are 0.54 and 0.51°, respectively, suggesting that the structures of films are reasonably good.

X-ray pole figure analysis was used to determine the orientation relationship between the films and the MgO substrates. The XRD pole figure plots of the $\{112\}$ reflections for both the BST films and MgO substrates are shown in fig. 2. For (001) BST films, two sets of peaks are expected to be seen in XRD pole figure by interplanar angles calculation. One set is 4 poles, $\alpha = 35.3^\circ$, $\beta = 90^\circ$ ((112) , $(\bar{1}\bar{1}2)$, $(1\bar{1}2)$, $(\bar{1}\bar{1}2)$), another set is 8 poles, $\alpha = 65.9^\circ$, $\beta = 36.9^\circ$ and 53.1° ((121) , $(\bar{1}21)$, $(1\bar{2}1)$, $(\bar{1}\bar{2}1)$, (211) , $(\bar{2}11)$, $(2\bar{1}1)$, $(\bar{2}\bar{1}1)$), coinciding with the experimental results and indicating alignment of the BST $\langle 001 \rangle$ and $\langle 100 \rangle$ parallel with the $\langle 001 \rangle$ and $\langle 100 \rangle$ of the substrate, respectively. For (011) BST films, two sets of peaks are expected to be seen in XRD pole figure by interplanar angles calculation. One set is 4 poles, $\alpha = 30^\circ$, $\beta = 70.5^\circ$ and 109.5° ((121) , $(\bar{1}21)$, (211) , $(\bar{2}\bar{1}1)$), Another set is 2 poles, $\alpha = 54.7^\circ$, $\beta = 180^\circ$ ((112) , $(\bar{1}\bar{1}2)$), coinciding with the experimental results and indicating alignment of the BST

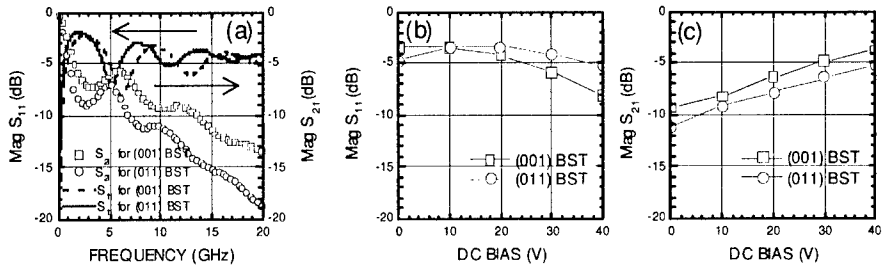


Figure 3. The measured microwave properties of the CPW device based on (001) and (011) BST films. (a) The losses as a function of frequency, (b) reflection loss (S_{11}), and (c) insertion loss (S_{21}) as a function of DC bias at 10 GHz for (001) and (011) BST films, respectively.

$\langle 011 \rangle$ parallel with the $\langle 011 \rangle$ of the substrate, which is equivalent with $\langle 100 \rangle_{\text{BST}} // \langle 100 \rangle_{\text{MgO}}$ and $\langle 001 \rangle_{\text{BST}} // \langle 001 \rangle_{\text{MgO}}$.

Figure 3 shows the measured microwave properties of the CPW device based on (001) and (011) BST films. Frequency dependant return loss (S_{11}) and insertion loss (S_{21}) of the CPW for (001) and (011) BST films at 0 V, respectively, are plotted in fig. 3 (a). The losses decrease with increasing applied DC bias field. The characteristic impedance of the CPW is not matched to that of the probes (50 Ω) resulting high return losses (S_{11}). Furthermore insertion loss (S_{21}) ranges -9.4 ~ -3.8 dB and -11.2 ~ -5.2 dB for (001) and (011) BST films, respectively, at 10 GHz with DC bias of 0 ~ 40 V, shown in fig. 3 (b) and (c). The values can be improved further by using a matched design.

The differential phase shift from 0V bias is shown in fig. 4 (a). As applied bias voltage and frequency increase, the differential phase shift also increase continuously. At the proposed operating frequency ranges (10 – 20 GHz), 63 ~ 122° and 94 ~ 183° of differential phase shift of S_{21} are observed with 40 V of a maximum applied DC bias voltage for (001) and (011) BST films, respectively. The applied DC bias voltage was limited by the commercial DC bias tees. However, the differential phase shift observed in the device is not saturated yet, which suggests that the differential phase shift will be increased further with a higher DC bias field.

Dielectric constants of the ferroelectric BST films are calculated from the phase value of S_{21} . First, phase length (ϕ) of the CPW can be expressed as following,

$$\phi_{21} = 2f_0 \sqrt{\epsilon_{\text{eff}} \mu_{\text{eff}}} \times l \times 180 / c, \text{----- (1)}$$

where f_0 is the operating frequency, ϵ_{eff} and μ_{eff} are the effective dielectric constant and magnetic permeability of CPW, respectively, l is the physical length of the CPW, and c is the light velocity in the air. Figure 4 (b) and (c) show total phase of S_{21} for the CPW and fitted results using eq. (1) when $\mu_{\text{eff}} = 1$ for (001) and (011) BST films on MgO substrates, respectively. To extract the dielectric constant of ferroelectric film, a modified conformal mapping technique has been used. Dielectric constant of substrate, film, and air has the following relation,

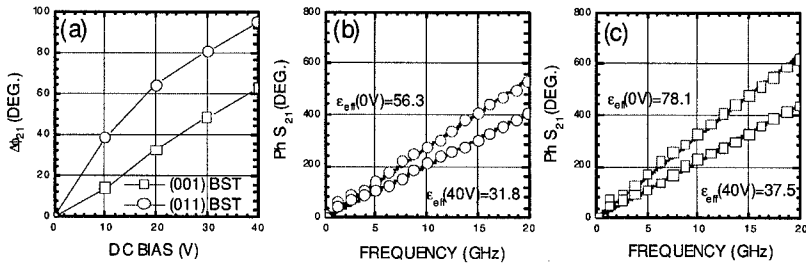


Figure 4. (a) Differential phase shift for (001) and (011) BST films at 10 GHz as a function of DC bias voltage, respectively. Total phase of S_{21} for (b) (001) BST films and (c) (011) BST films as a function of frequency with DC bias 0 and 40 V and linear fitting to extract effective dielectric constant of CPW. The open symbols indicate the measured data, the lines indicate the fitting results.

$$\epsilon_{eff} = k_{sub}\epsilon_{sub} + k_{film}\epsilon_{film} + k_{air}\epsilon_{air}, \text{-----}(2)$$

where k_i corresponds to the filling factors for the substrate, film and air, respectively. The calculated film dielectric constant decreases from 1400 and 2000 at 0 V to 750 and 900 at 40 V for (001) and (011) BST, respectively. This is corresponding to 46 % and 55 % of dielectric constant tunability with less than 70 kV/cm for (001) and (011) BST, respectively, which is comparable with those of the reported BST films. This suggest that the dielectric constant tunability of (011) BST films is larger than that of (001) BST films. Furthermore, to achieve larger differential phase angle, CPW on (011) BST might have advantage over that on (001), since BST on (011) has larger dielectric constant and larger tunability at the same time than that on (001). More test results with matched CPW will be studied in a future.

CONCLUSIONS

In summary, coplanar waveguide-type phase shifters were fabricated on (001) and (011) BST films. Under DC bias field, the measured differential phase shift and insertion loss (S_{21}) in the device on (011) BST films are larger than those in the device on (001) BST films. The calculated film dielectric constants and dielectric constant tunability for (011) BST films are also larger than those for (001) BST films.

ACKNOWLEDGMENTS

We gratefully acknowledge the support from the Minister of Information and Communication Department of Korea. The authors thank Dr. M. H. Kwak for helpful discussions.

REFERENCES

1. M. J. Lancaster, J. Powell, and A. Porch, *Supercond. Sci. Technol.* **11**, 1323 (1998).
2. J. V. Mantese, N. W. Schubring, A. L. Micheli, A. B. Catalan, M. S. Mohammed, R. Naik, and G. W. Auner, *Appl. Phys. Lett.* **71**, 2047 (1997).
3. W. Chang, C. M. Gilmore, W. J. Kim, J. M. Pond, S. W. Kirchoefer, S. B. Qadri, D. B. Chirsey, and J. S. Horwitz, *J. of Appl. Phys.* **87**, 3044 (2000).
4. F. W. Van Keuls, C. H. Mueller, F. A. Miranda, R. R. Romanofsky, C. L. Canedy, S. Aggarwal, T. Venkatesan, R. Ramesh, J. S. Horwitz, W. Chang, and W. J. Kim, *IEEE MTT-S* **2**, 737 (1999).
5. S. Jun, Y. S. Kim, Y. W. Kim, and J. Lee, *Appl. Phys. Lett.* **78**, 2542 (2001).
6. C. M. Carlson, T. V. Rivkin, P. A. Parilla, J. D. Perkins, D. S. Ginley, A. B. Kozyrev, V. N. Oshadchy, and A. S. Pavlov, *Appl. Phys. Lett.* **76**, 1920 (2000).
7. C. L. Canedy, S. Aggarwal, H. Li, T. Venkatesan, R. Ramesh, F. W. Van Keuls, R. R. Romanofsky, and F. A. Miranda, *Appl. Phys. Lett.* **77**, 1523 (2000).
8. E. G. Erker, A. S. Nagra, Y. Liu, P. Periaswamy, T. R. Taylor, J. Speck, and R. A. York, *IEEE Micro. And Guided Wave Lett.* **10**, 10 (2000).
9. B. H. Park, E. J. Peterson, Q. X. Jia, J. Lee, X. Zeng, W. Si, and X. X. Xi, *Appl. Phys. Lett.* **78**, 533 (2001).
10. W. Chang, J. S. Horwitz, W. J. Kim, J. M. Pond, S. W. Krichoefer, C. M. Gilmore, S. B. Qadri, and D. B. Chrisey, *Mat. Res. Soc. Symp. Proc.* **541**, 699 (1999).
11. L. C. Sengupta, E. Ngo, M. E. O'Day, S. Stowell, and R. Lancto, *ISAF '94. Proceedings of the Ninth IEEE International Symposium on Applications of Ferroelectrics* 622 (1995).
12. W. J. Kim, W. Chang, S. B. Qadri, J. M. Pond, S. W. Krichoefer, D. B. Chrisey, and J. S. Horwitz, *Appl. Phys. Lett.* **76**, 1185 (2000).
13. W. Chang, J. S. Horwitz, W. J. Kim, J. M. Pond, S. W. Krichoefer, C. M. Gilmore, S. B. Qadri, and D. B. Chrisey, *Mat. Res. Soc. Symp. Proc.* **541**, 693 (1999).
14. W. J. Kim, W. Chang, S. B. Qadri, J. M. Pond, S. W. Kirchoefer, J. S. Horwitz, and D. B. Chrisey, *Appl. Phys. A* **70**, 313 (2000).
15. S. S. Gevorgian, T. Martinsson, P. I. J. Linnér, and E. L. Kollberg, *IEEE Trans. Microwave Theory Tech.* **44**, 896 (1996).
16. E. Carlsson, and S. Gevorgian, *IEEE Trans. Microwave Theory Tech.* **47**, 1544 (1999).